Saharan dust effects on North Atlantic sea-surface skin temperatures

PIRATA-24/TAV Meeting

Bingkun Luo, Peter J. Minnett, Paquita Zuidema
Rosenstiel School of Marine and Atmospheric Science, University of Miami
Nicholas R. Nalli *IMSG, Inc. at NOAA/NESDIS/STAR*
Santha Akella *NASA Goddard Space Flight Center, Global Modeling and Assimilation Office (GMAO)*

CONTENTS

01

PART ONE

Introduction and Data

Significance of this study

- Saharan dust outbreaks frequently propagate westward over the Atlantic Ocean; accurate quantification of the dust aerosol scattering and absorption effect on the surface radiative fluxes (SRF) is fundamental to understanding critical climate feedbacks.

- Accurate independent shipboard measurements in the tropical Atlantic Ocean area provide an independent representation of the atmosphere and ocean that can be used to investigate the influence of the dust aerosols on skin Sea-Surface Temperature (SSTskin) variability.

- This study includes the RRTMG-simulated surface shortwave and net longwave downwelling radiative changes due to dust and calculates the corresponding thermal skin layer temperature changes.

UNIVERSITY
OF MIAMI
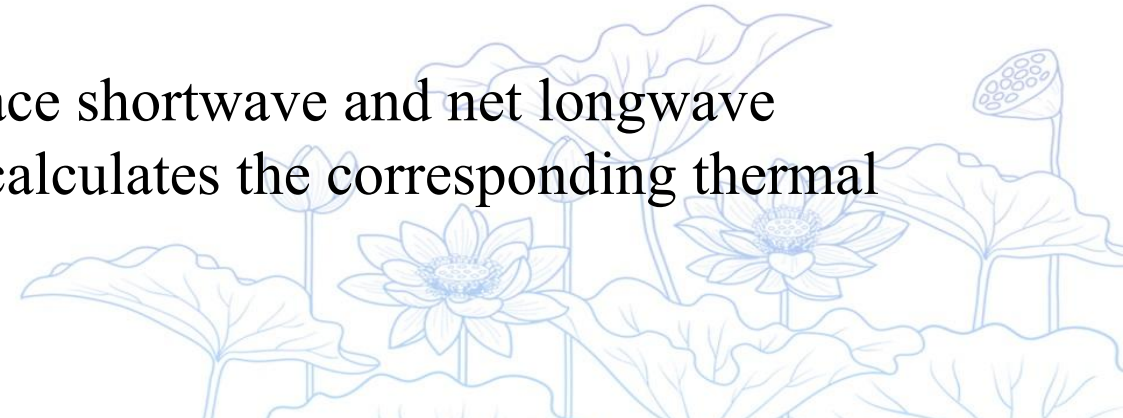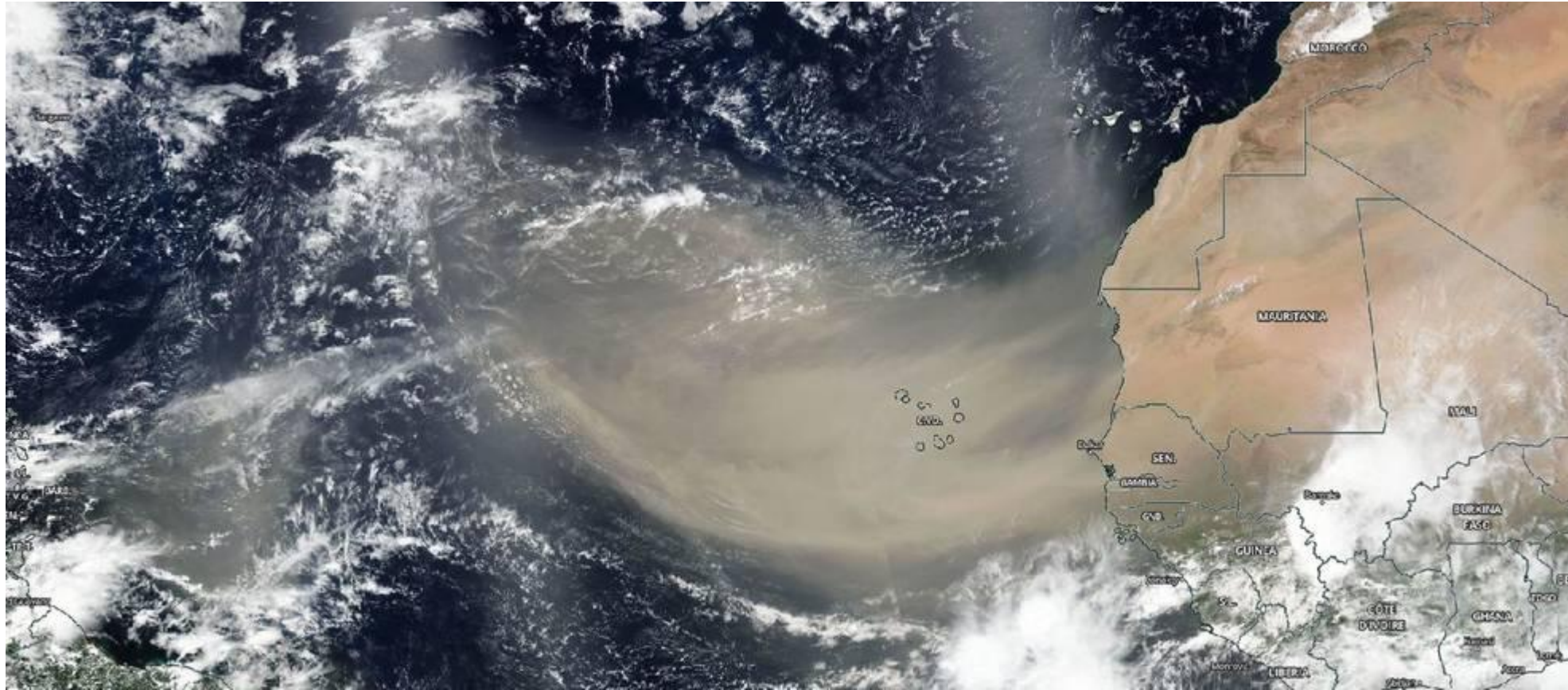
A massive dust plume from the Sahara Desert reaches far out over the Atlantic Ocean from the NASA-NOAA Suomi NPP Earth-observing satellite on June 13, 2020. (Image credit: NASA Worldview at https://www.nasa.gov/feature/goddard/2020/nasa-observes-large-saharan-dust-plume-over-atlantic-ocean)

"True-color" composite image of the Saharan Dust plume captured by the VIIRS instrument aboard NASA/NOAA's Suomi NPP satellite on June 24, 2020. The bright streaks seen at regular intervals are due to sun glint off of the ocean surface. (Image credit: https://www.nasa.gov/feature/goddard/2020/nasa-noaa-s-suomi-npp-satellite-analyzes-saharan-dust-aerosol-blanket)

Aerosols and Ocean Science Expeditions (AEROSE) tracks
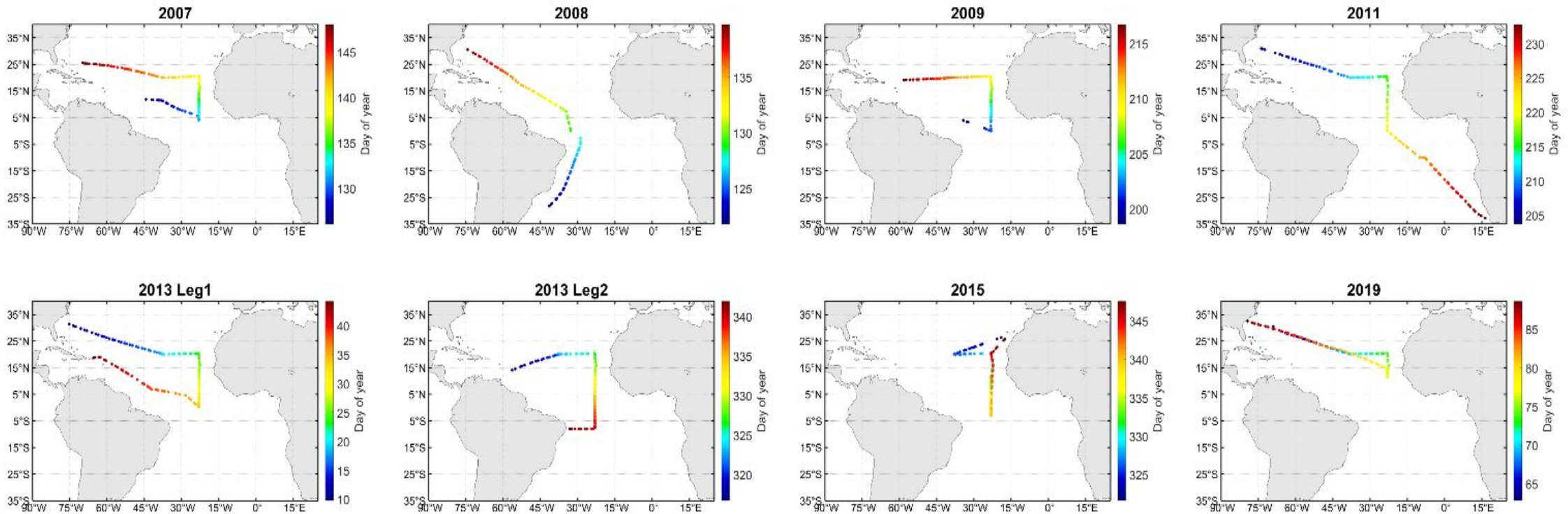
Color indicates the days since departure

Nalli, N.R., Joseph, E., Morris, V.R., Barnet, C.D., Wolf, W.W., Wolfe, D., Minnett, P.J., Szczodrak, M., Izaguirre, M.A., Lumpkin, R., Xie, H., Smirnov, A., King, T.S., & Wei, J. (2011). Multiyear Observations of the Tropical Atlantic Atmosphere: Multidisciplinary Applications of the NOAA Aerosols and Ocean Science Expeditions. Bulletin of the American Meteorological Society, 92, 765-789

Shipboard SST dataset

The M-AERI is an accurate, self-calibrating, Fourier transform IR spectroradiometer that measures emission spectra from the sea and atmosphere (Minnett et al. 2001).

M-AERI onboard the Ronald H. Brown.

NOAA Ship R.H.B at Florida. Mar 2 2018

M-AERI is calibrated in the laboratory before and after each deployment using an external validation procedure.

UNIVERSITY OF MIAMI

Shipboard Radiosonde dataset

Launching RS92 radiosonde 30 min prior to satellite sounder overpass. (Nalli et al. 2011)

| CRUISES	NUMBER OF RADIOSONDES	START	END	DAYS OF DATA
2007	96	2007-05-07	2007-05-28	22
2008	74	2008-04-29	2008-05-19	21
2009	78	2009-07-11	2009-08-11	31
2011	102	2011-07-21	2011-08-20	31
2013 Leg 1	111	2013-01-09	2013-02-13	36
2013 Leg 2	97	2013-11-11	2013-12-08	28
2015	92	2015-11-17	2015-12-14	28
2019	101	2019-02-24	2019-03-29	34
Total	**751**	**2007-05-07**	**2019-03-29**	**231**

Shipboard Radiosonde measurements
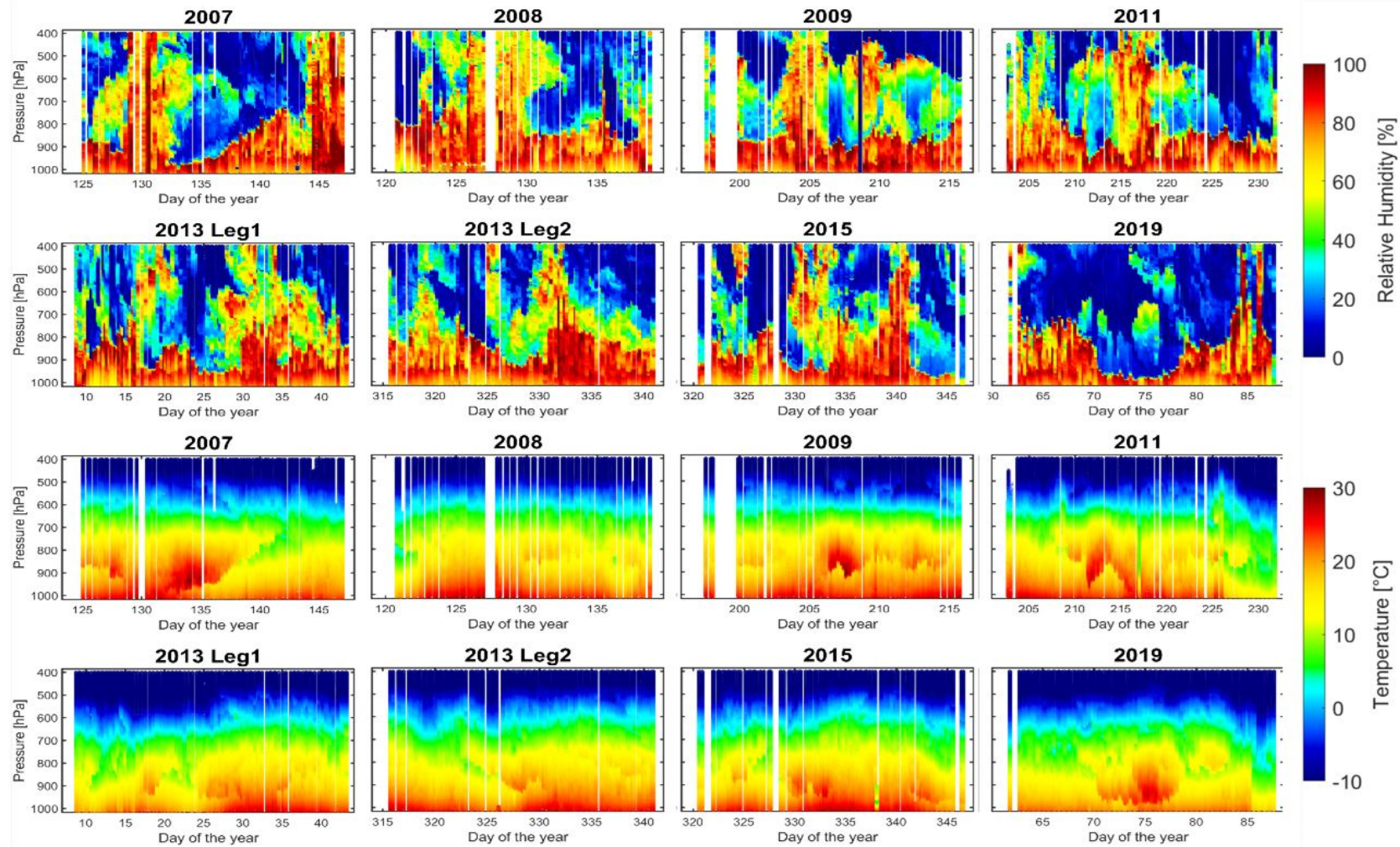
MERRA-2 reanalysis value

NASA Modern-Era Retrospective analysis for Research and Applications, Version 2 (MERRA-2) three-dimensional aerosol dust concentrations
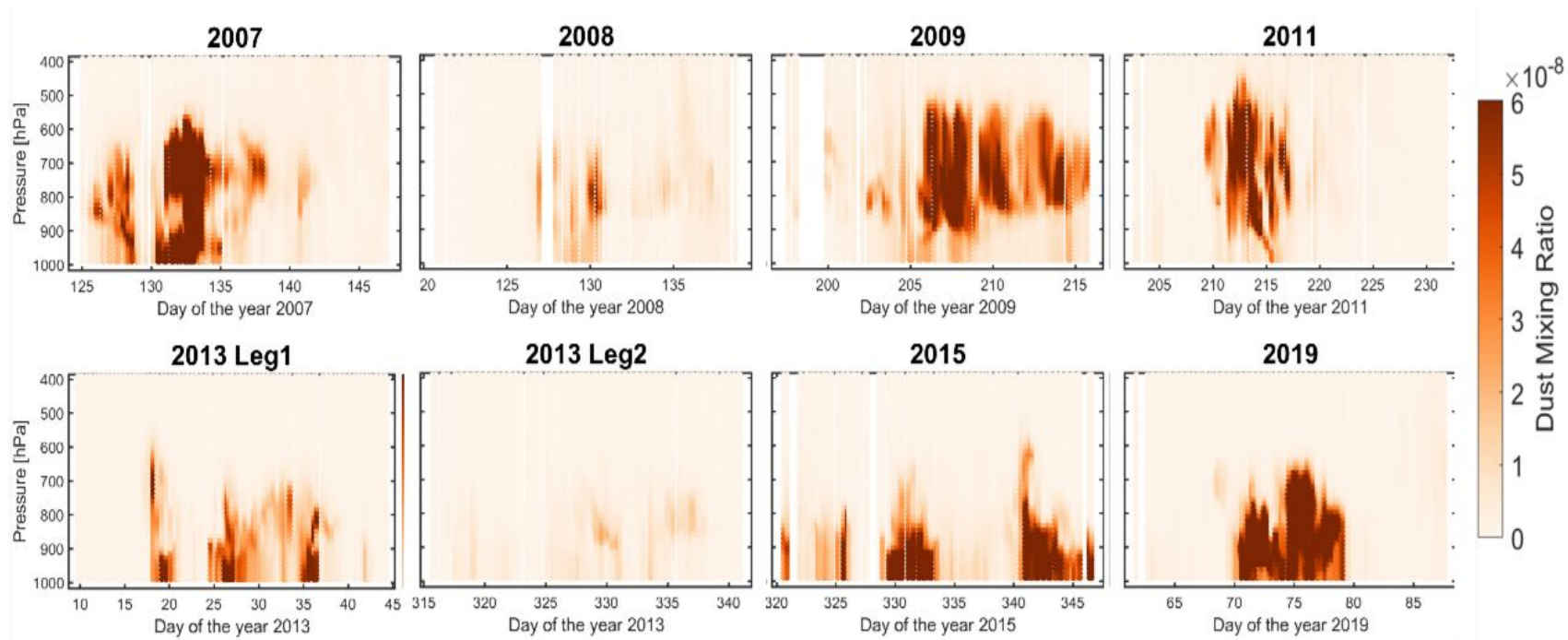
Gelaro, Ronald, et al. "The modern-era retrospective analysis for research and applications, version 2 (MERRA-2)." Journal of Climate 30.14 (2017): 5419-5454.

02

PART TWO

Net radiative effects of dust at the ocean surface (the tropical North Atlantic)

Significance of this study

- Accurate quantification of the surface radiative fluxes (SRF) is fundamental to understanding critical climate feedbacks and the Earth's surface energy budget.

- Current global SRF datasets are calculated using radiative transfer models with inputs from satellite observations and reanalysis fields.

- Oceanic SRF can be improved under the abnormal atmospheric cases such as under aerosol effect by combining independent observations.

- By exploiting large sets of measurements from many ship campaigns in conjunction with reanalysis products, this study characterizes the sensitivity of the SRF to the Saharan dust aerosols using radiative transfer models.

UNIVERSITY
OF MIAMI
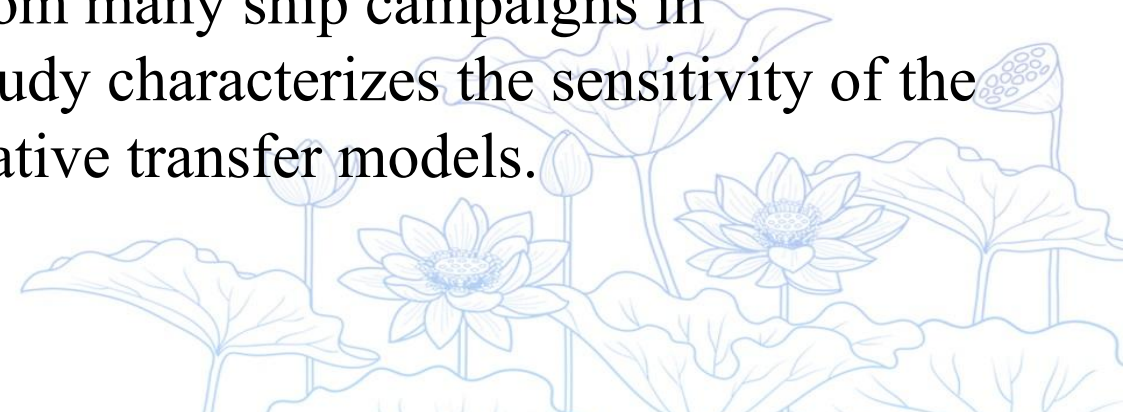
Introduction of this study

- The Rapid Radiative Transfer Model for General Circulation Models Applications (RRTMG) was used

- The field data are measurements of the M-AERI SST_{skin}, and vertical atmospheric temperature and water vapor radiosonde profiles. The aerosol dust concentrations from the NASA MERRA-2.

Aerosol optical depth of each layer

Atmospheric layer thickness

$$\tau^j = \sum_z x_i \times b_{ex}(RH, \lambda) \times \delta z$$

MERRA-2 dust mixing ratio

TABLE 1. Aerosol optical properties by species at $\lambda = 0.55$ μm and as a function of relative humidity (RH).[a]

| Species	Mass Extinction Coefficient[e] (β_{ext}) [m^2 g^{-1}]			Single Scattering Albedo[f] (ω_o)			Asymmetry Parameter[g] (g)		
	RH = 0%	RH = 80%	RH = 95%	RH = 0%	RH = 80%	RH = 95%	RH = 0%	RH = 80%	RH = 95%
Dust Bin 1[b]	2.02	2.02	2.02	0.96	0.96	0.96	0.71	0.71	0.71
Dust Bin 2[b]	0.64	0.64	0.64	0.92	0.92	0.92	0.75	0.75	0.75
Dust Bin 3[b]	0.33	0.33	0.33	0.89	0.89	0.89	0.80	0.80	0.80
Dust Bin 4[b]	0.17	0.17	0.17	0.83	0.83	0.83	0.84	0.84	0.84
Dust Bin 5[b]	0.08	0.08	0.08	0.77	0.77	0.77	0.87	0.87	0.87
Sea Salt Bin 1[c]	0.73	4.54	25.98	1.00	1.00	1.00	0.20	0.50	0.69
Sea Salt Bin 2[c]	3.48	10.01	24.02	1.00	1.00	1.00	0.70	0.78	0.79
Sea Salt Bin 3[c]	0.74	2.04	4.85	1.00	1.00	1.00	0.71	0.78	0.83
Sea Salt Bin 4[c]	0.30	0.86	2.02	1.00	1.00	1.00	0.77	0.83	0.85
Sea Salt Bin 5[c]	0.10	0.30	0.72	1.00	1.00	1.00	0.81	0.86	0.87
Hydrophobic BC[d]	9.28	9.28	9.28	0.21	0.21	0.21	0.33	0.33	0.33
Hydrophilic BC[d]	9.28	11.27	15.77	0.21	0.25	0.38	0.33	0.40	0.50

$$\alpha = \sum_i \alpha_i;$$

$$\omega = \frac{\sum_i \alpha_i \omega_i}{\sum_i \alpha_i},$$

$$g = \frac{\sum_i \alpha_i \omega_i g_i}{\sum_i \alpha_i \omega_i},$$

Ref:
Thorsen, T. J., Ferrare, R. A., Kato, S., & Winker, D. M. (2020). Aerosol direct radiative effect sensitivity analysis. *Journal of Climate*, *33*(14), 6119-6139.
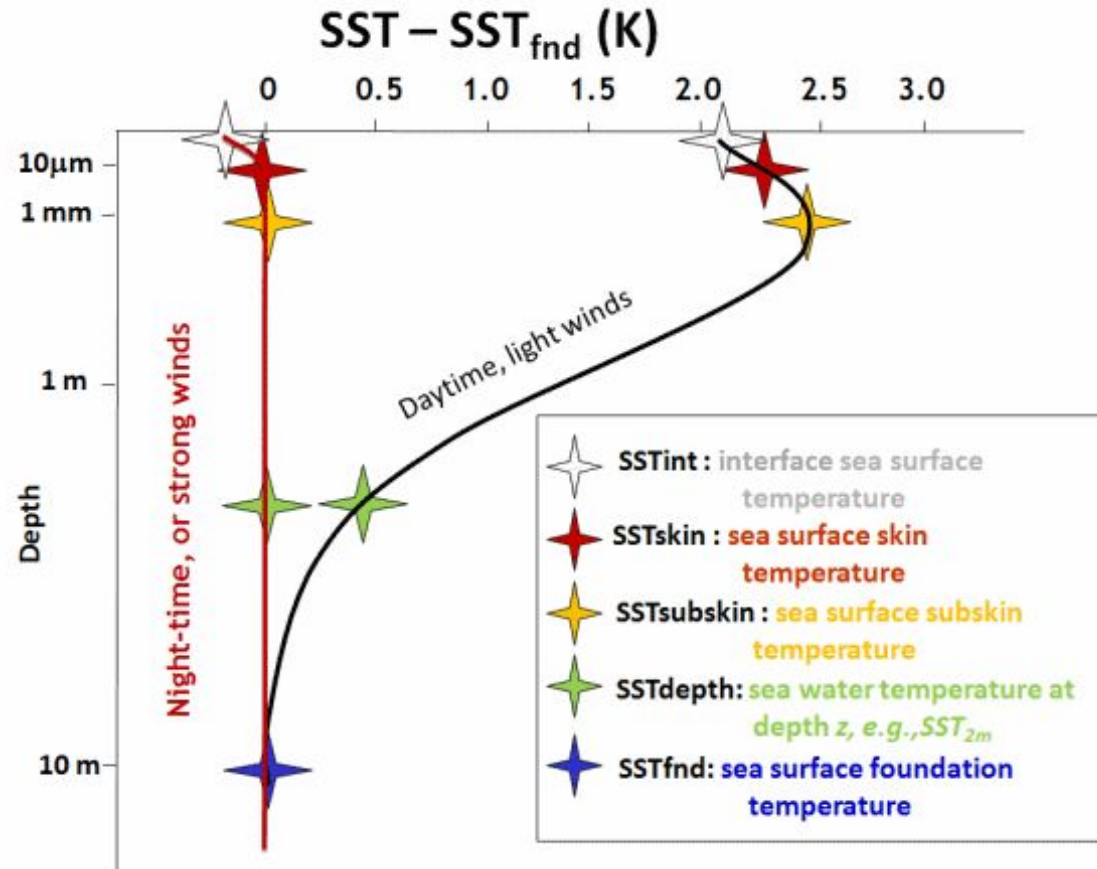
UNIVERSITY
OF MIAMI
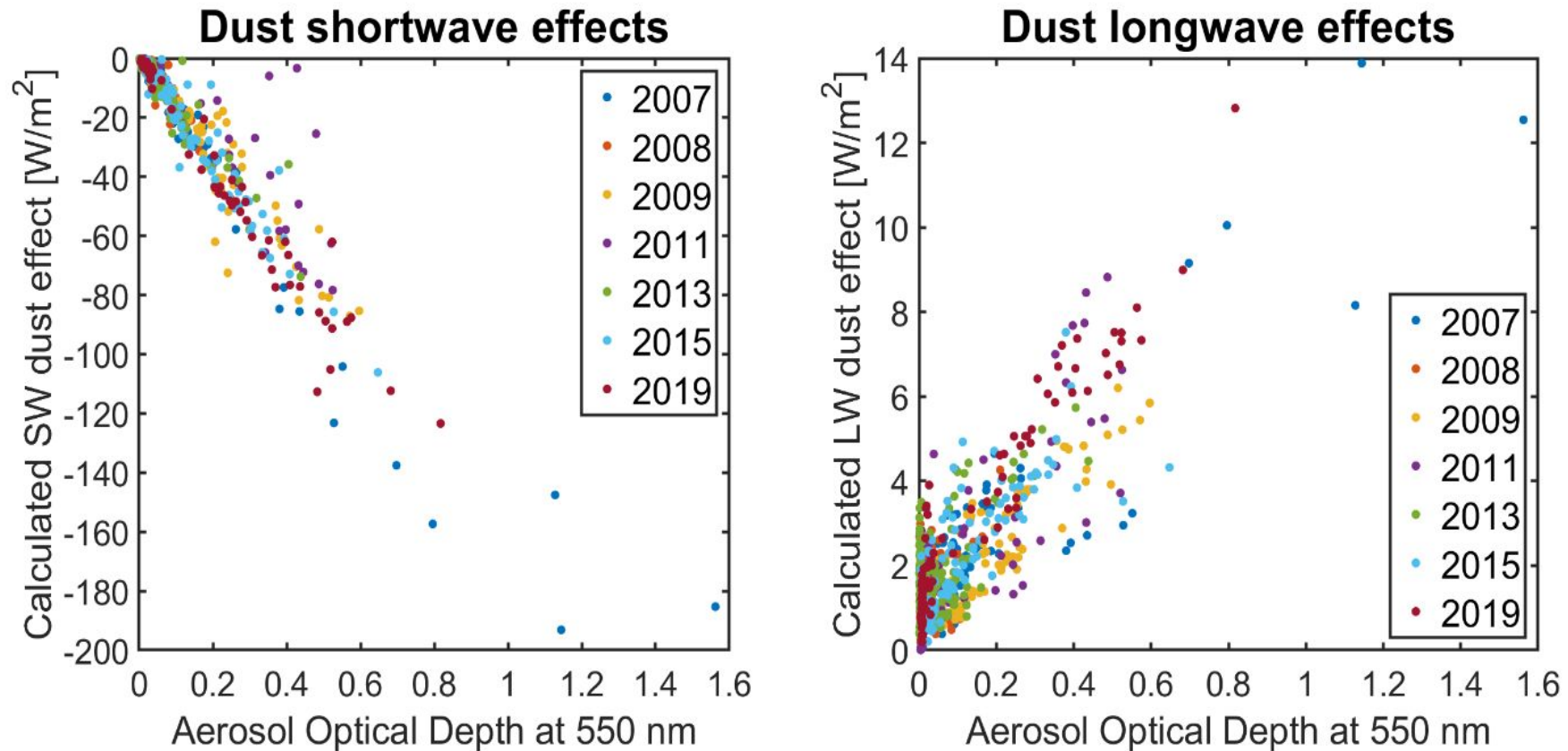
Left: RRTMG calculated Saharan dust shortwave effects at sea surface with AOD at 550 nm for the radiosonde deployment stations. Right: RRTMG calculated Saharan dust longwave effects. The colors indicate the deployment year.
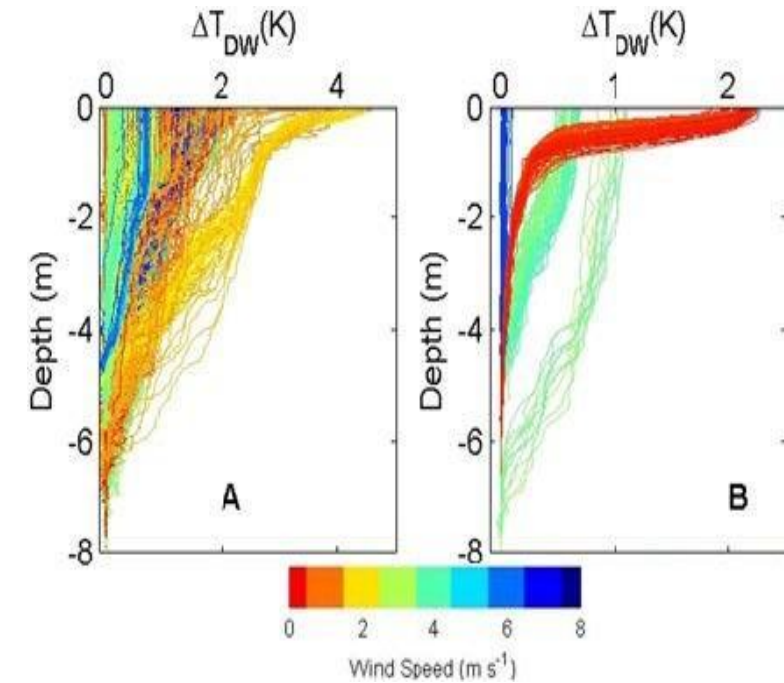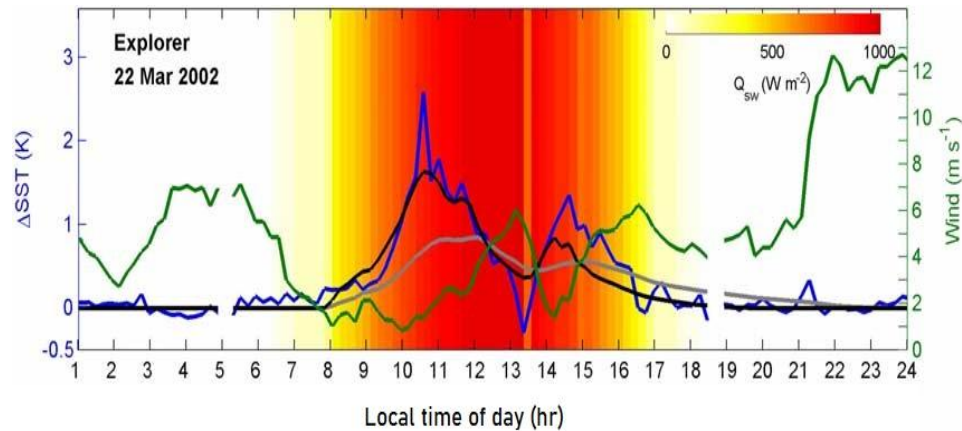
03

PART THREE

SST_{skin} response to dust radiative effects

UNIVERSITY
OF MIAMI

A schematic drawing of ocean near-surface vertical temperature profile during nighttime and daytime. Variability exists in both the temperature and depth scales. Taken from: https://www.ghrsst.org/ghrsst-data-services/products/

The diurnal heating signal (SST$_{skin}$ – TTSG) in blue. Insolation is background, wind speed the green line (right axis), Simulations of Fairall et al., (1996) are the gray line, and Gentemann et al., (2009) are the black line.

Upper ocean temperature profiles colored by wind speed at the time of the profile (A). A smoothed subset showing the clear wind-speed dependence (B). From Gentemann et al., (2009).

Gentemann, C. L., Minnett, P. J., & Ward, B. (2009). Profiles of ocean surface heating (POSH): A new model of upper ocean diurnal warming. *Journal of Geophysical Research: Oceans*, *114*(C7).

UNIVERSITY
OF MIAMI

Diurnal SST$_{skin}$ model by Akella et al. 2017; ECMWF 2016; Gentemann and Akella 2018; Takaya et al. 2010; Zeng and Beljaars 2005:

$$SST_{skin} = SST_{fnd} - \Delta SST_d + \Delta SST_W(z) \qquad (1)$$

where SST_{fnd}, ΔSST_d and ΔSST_W are OSTIA SST_{fnd}, diurnal warming and cool-skin temperature changes respectively. The cool skin effect, the temperature difference between SST_{skin} and SST_{fnd} can be expressed as:

$$SST_{skin} - SST_{fnd} = \frac{\delta}{\rho_w c_w k_w}(Q_c) \qquad (2)$$

where ρ_w is the water density, c_w is the volumetric heat capacity, k_w is the molecular thermal conductivity of water and δ is the skin layer thickness. Q_c is the net heat flux through the sea surface:

$$Q_c = H_s + H_L - LW_{net} - f_s SW_{net}^c \qquad (3)$$

where H_s, H_L, and LW_{net} denote the sensible heat flux, latent heat flux and net long wave radiation at the surface. SW_{net}^c is the net solar radiation at the surface, f_s is the fraction of the surface-absorbed solar radiation within the near surface ocean, given by Fairall et al. (1996).

From RRTMG simulations
With and without dust

The diurnal warming calculations are based on Takaya et al. (2010) and can be expressed as:

$$\frac{\partial(SST_{-\delta}-SST_{fnd})}{\partial t} = \frac{Q_w+R_s-R(-d)}{d\rho_w c_w \nu/(\nu+1)} - \frac{(\nu+1)ku_{*w}}{d\phi_t(d/L)}\left(SST_{-\delta} - SST_{fnd}\right) \quad (4)$$

where $SST_{-\delta}$ is the temperature below the cool skin layer, d is the depth of the diurnal warm layer, which is set as 3 m, ν is the profile shape and it is set as 0.3, u_{*w} is the water friction velocity, $\phi_t(d/L)$ is the stability function and L is the Obukhov length; $R(-d)$ is the solar radiation absorbed at depth -d. The net heat flux at the surface available to heat the warm layer, Q_w, is given by:

$$Q_w \rightarrow SW_{net}^w + LW_{net} - H_s - H_L \quad (5)$$

From RRTMG simulations With and without dust

From most updated version v3.6 of the Tropical Ocean and Global Atmosphere Coupled Ocean–Atmosphere Response Experiment (TOGA COARE)

Note the SW_{net}^w is net short-wave radiation absorbed in the warm layer, $SW_{net}^w = SW_{net}^c - SW_{PEN}$, where SW_{PEN} is the penetrating short-wave radiation that can be obtained from the three-band absorption profile of Soloviev and Vershinsky (1982) the coefficients a_i and b_i can be obtained from Zeng and Beljaars (2005).

$$SW_{PEN} = SW_{net}^c \sum_{i=1}^{N=3} a_i \, exp\,(-db_i) \quad (6)$$

Equation (4) has been integrated in time to derive the warm layer effect; during daytime, the warm layer effect $(T_{-\delta} - T_{fnd})$ from Equation (4) and the cool layer effect $(T_{skin} - T_{fnd})$ from Equation (2) have been added together to derive T_{skin}.

UNIVERSITY
OF MIAMI

SSTskin change due to dust

SSTskin change due to dust
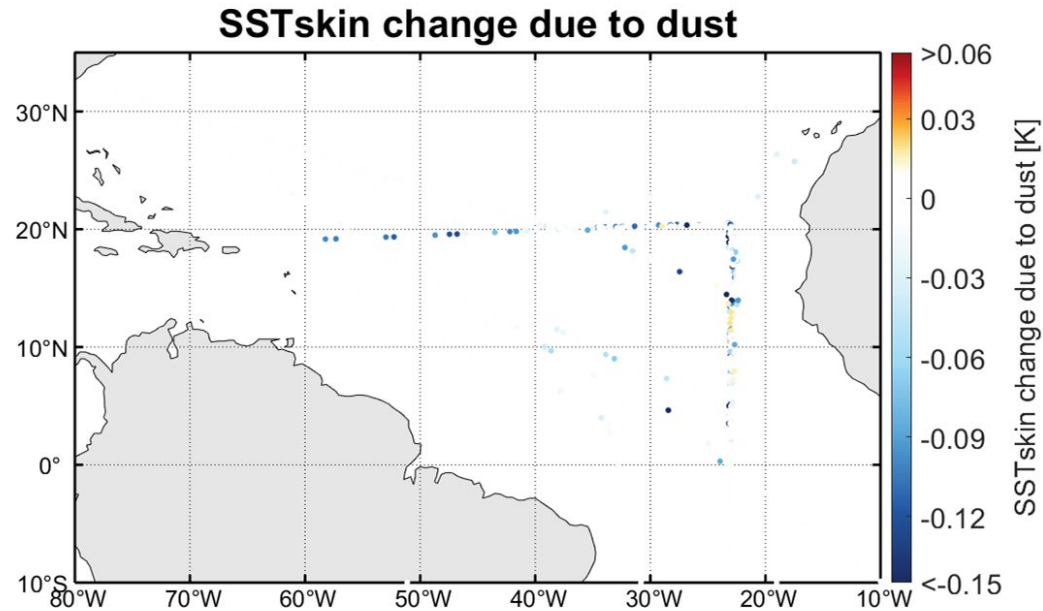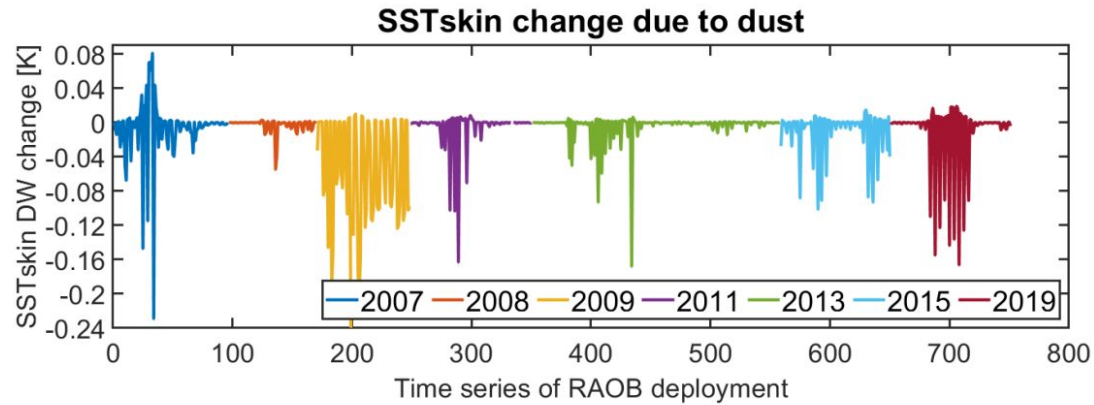
Top: Time series of the SST_{skin} changes due to dust. The x-axis is the radiosonde deployment number, and the y-axis shows the simulated SST_{skin} changes, which are calculated as the difference between the SST_{skin} with and without dust. The unit is K. The colors indicate the deployment year. Bottom: Geographic distributions of the calculated SST_{skin} changes due to dust. The colors indicate the SST_{skin} change due to dust, as shown on the right with the unit of K. Note there are many points which have almost zero SST_{skin} change.

UNIVERSITY
OF MIAMI
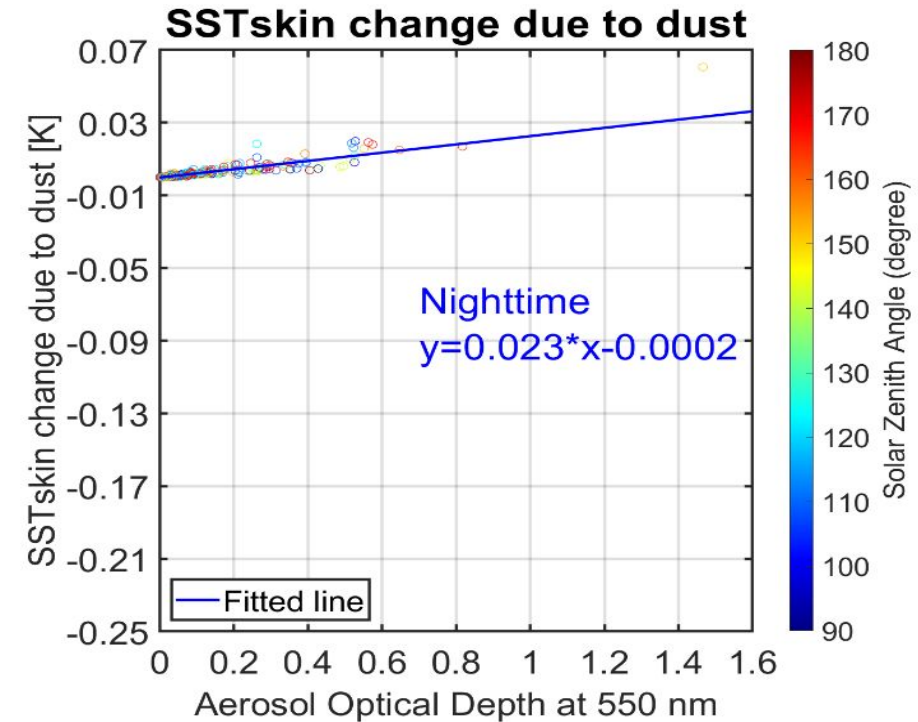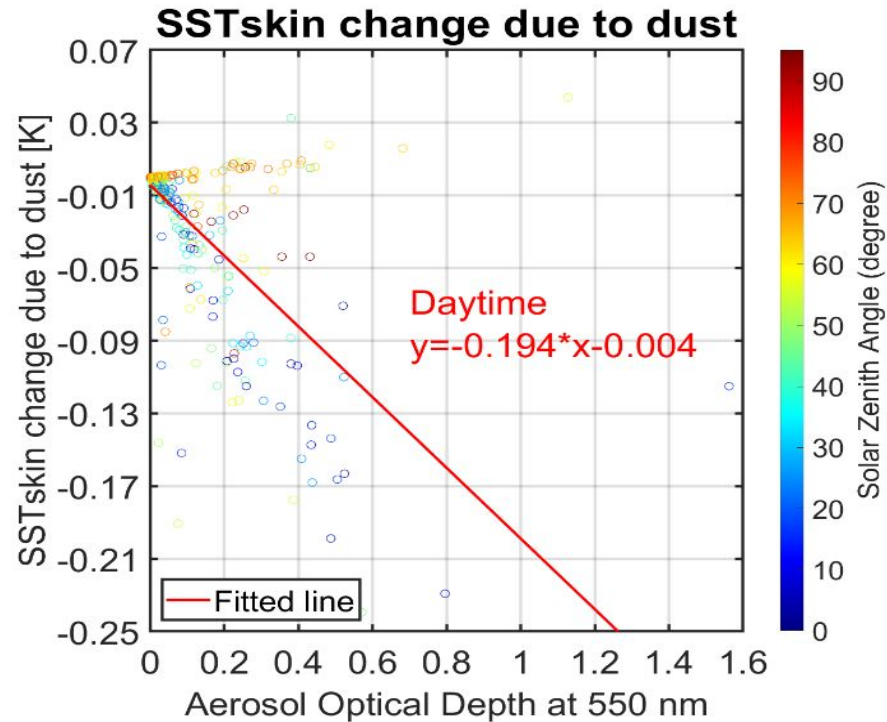
Left: Calculated daytime SST_{skin} changes due to dust with AOD at 550 nm, the SST_{skin} changes are large with high aerosol concentrations. Right: Calculated nighttime SST_{skin} changes.

05

PART FIVE
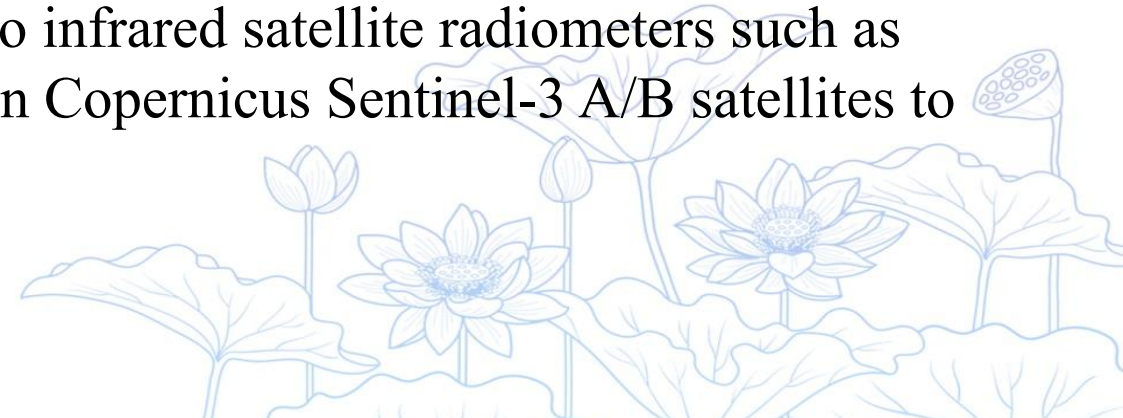
Conclusions & Future Work

UNIVERSITY
OF MIAMI

Conclusions:

•By exploiting large sets of measurements from many ship campaigns in conjunction with reanalysis products, this study characterizes the sensitivity of the SRF and SSTskin to the Saharan dust aerosols using models of the atmospheric radiative transfer and thermal skin effect.

•The dust outbreaks can decrease the surface shortwave radiation up to 190 W/m^2 and increase the surface longwave radiation by up to 14W/m^2.

•SSTskin response to the abnormal surface radiative fluxes can range from a net cooling to a tiny warming: -0.24K to 0.06K.

•Greater physical insight into the radiative transfer through an aerosol-burdened atmosphere will substantially improve the predictive capabilities of weather and climate studies on a regional basis.
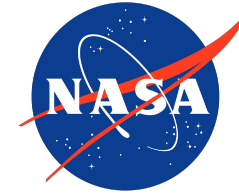
UNIVERSITY
OF MIAMI
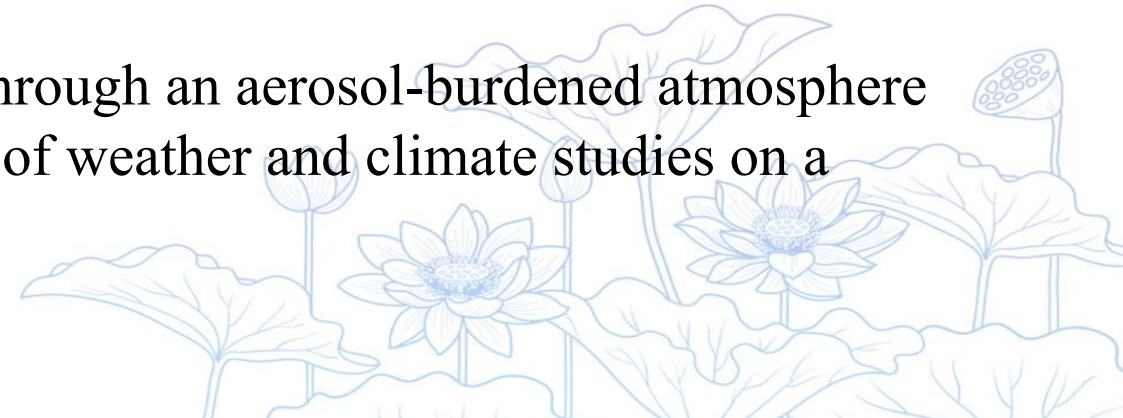
Future Work:

- Since reanalyses (e.g., MERRA-2) capture detailed aerosol variability, how does that impact brightness temperature simulation? And in-turn, does that impact meteorological assimilation?
- We also recommend that more detailed determination of the dust effects on SRF requires better knowledge of dust radiative properties and vertical distribution of aerosol layers derived, for example, from ship-based lidar or from CALIPSO satellite.
- The impact of different kinds of aerosol layers should be further explored.
- Such approaches as developed here can be applied to infrared satellite radiometers such as VIIRS on the Suomi-NPP and NOAA-20, SLSTR on Copernicus Sentinel-3 A/B satellites to improve the SSTskin retrieval.

Thank you.

THANK YOU!

Bingkun Luo and Peter Minnett
Rosenstiel School of Marine and Atmospheric Science
University of Miami
LBK@rsmas.miami.edu